Another remarkable observation on Figure 2 is the shift of the maximum of sensitivity to the oxygen-rich side with the tetranitromethane-nitromethane mixtures. If the card number is plotted as a function of enthalpy of explosion in Figure 4, it is seen that peak sensitivity appears at peak enthalpy (1600 cal. per gram) except with the oxygen-rich branch of tetranitromethane-nitromethane, where a somewhat higher sensitivity is reached at 1100 cal. per gram. Note that the sensitivity increase at the enthalpy of nitromethane (960 cal. per gram) is more than fourfold.

In general, the chemical constitution has a great influence on shock sensitivity in accord with experience at other places. Tests on more types of mixtures appear to be worth while.

LITERATURE CITED

(1) American Rocket Society, Committee on Monopropellant Test Methods, Recommended Test No. 1, Card Gap Test for Shock Sensitivity of Liquid Monopropellants, July 12, 1955.
(2) Hager, K. F., *Ind. Eng. Chem.* 41, 2168 (1949).
(3) Hefco Labs., Inc., Detroit, Mich., "Technical Report on Rocket Fuels," Office of Naval Research Project 22001g (May–December 1948).
(4) Tschinkel, J. G., *Ind. Eng. Chem.* 48, 732 (1956).

Received August 29, 1957. Accepted January 17, 1958.

Volume Changes in Petroleum Waxes as Determined from Refractive Index Measurements

DONALD V. HARRISON, ALFRED M. REINGOLD, and WILLIAM R. TURNER
The Atlantic Refining Co., Research and Development Department, Philadelphia, Pa.

Solid transitions take place in commercial paraffin waxes as well as in pure *n*-paraffin hydrocarbons, and these changes can be detected in a variety of ways (*13, 14, 20, 21, 25, 26*). The changes in translucency, mottling, and formation of bubbles that occur in masses of paraffin wax during storage are evidences that basic changes in structure are taking place.

The volume changes accompanying such transitions are of considerable importance in commercial applications for waxes. For example, in the molding of candles, contraction must be carefully controlled, if the candles are to release from the mold properly, and yet not contain stresses which will make them unduly fragile in handling. The cracking of wax films on paper food cups and milk containers as a result of thermal shocks which accompany the processing of the containers is a further example of the practical importance of volume changes in solid waxes.

Therefore, in the formulation of waxes for specific end uses a convenient method is needed for measuring volume changes with respect to temperature.

The direct method is to measure changes in volume as they occur with variations in temperature, using apparatus such as the dilatometer (*24*). The chief difficulties in using the dilatometer lie in the need for completely removing and excluding gases from the solid sample and in the lengthy periods of time needed to bring the system to equilibrium. Certain other methods, such as those involving measurement of dielectric constant, or x-ray diffraction, permit the calculation of wax volume, but are too complex for everyday use.

Described here is a method by which volume changes in petroleum waxes may be estimated over a range of temperatures with sufficient ease and accuracy to warrant its use in the development of wax products. The method uses a density determination in the liquid state together with measurements of refractive index in both liquid and solid states, to provide the data needed to calculate density or specific volume at other temperatures.

METHOD OF CALCULATION

The fact that a relationship exists between density and refractive index of a material permits calculation of density and of specific volume at any temperature from easily obtained measurements of the refractive index at that temperature and of the density and refractive index at one temperature in the liquid state. Johnson (*13*) has successfully used this relationship to measure transition temperature ranges in paraffin waxes, and to determine densities of liquid and solid dotriacontane.

The expression of this relationship showing closest agreement with observation over the range of temperatures considered here is given by the formula of Lorentz and Lorenz:

$$r = \frac{n^2 - 1}{n^2 + 2} \times \frac{1}{d} \qquad (1)$$

where r is the specific refractivity in terms of n, the refractive index, and d, the density at the same temperature.

The specific refractivity has been shown to be considered substantially independent of the state of aggregation and relatively invariant to change in temperature (*10, 11, 16*). Thus, the density at any temperature may be calculated from the refractive index at that temperature and the specific refractivity. The specific refractivity is most easily calculated from refractive index and density at a temperature where the wax is liquid.

By equating the expressions for specific refractivity at the two temperatures, the density at the second temperature can be calculated. It is given by

$$d_2 = d_1 \left(\frac{n_1^2 + 2}{n_1^2 - 1}\right)\left(\frac{n_2^2 - 1}{n_2^2 + 2}\right) \qquad (2)$$

where d_1 and d_2 are the densities at the two temperatures, and n_1 and n_2 are the refractive indices at the same two temperatures.

In practical application it is usually more convenient to speak in terms of volume rather than of density changes taking place in a wax. Accordingly in the cases which follow, specific volume, the reciprocal of the density, has been shown in addition to or instead of density.

As solid petroleum wax is known to be birefringent, a mean value for refractive index must be calculated for use in Equation 2. Although strict adherence to the theory requires the use of a geometric mean, in practice the approximation given by Pope (*18*)

$$n = \frac{2n_o + n_e}{3} \qquad (3)$$

is sufficiently accurate for most work. Here n_o and n_e represent the refractive indices as given by the ordinary and extraordinary rays, respectively.

In this work no correction of the observed refractive indices was made, as the main interest was comparison and not absolute values.

Table I. Physical Test Data

Test		Wax A	B	C	D	E	F	G	H
Melting point, °F. (ASTM D 87–42)		129.8	128.7	143.8	171.6[a]	143.4	143.1	143.3	124.2
Melting point, °F. (By refractive index)		129.2	129.2	143.6	168.8	143.6	142.9	143.6	124.5
Oil content, % (ASTM D 721–56T)		1.1	0.5	0.7	1.0	0.6	0.8	1.7	0.3
Refractive index, at 176°F.		1.4268	1.4282	1.4306	1.4481	1.4315	1.4351	1.4311	1.4286
Transition range, °F.	Top	107.6	104.0	118.4	.....[b]	119.3	122.0	120.2	96.8
	Mid-point	106.9	92.0	117.5	.....	116.2	114.8	116.4	84.6
	Bottom	106.2	77.0	116.6	.....	105.8	105.8	104.0	71.6
Penetration (ASTM D 1321)									
77°F.		12	14	11	13	10	9	14	21
90		17	38	15	20	13	12	19	58
100		25	96	19	25	17	16	22	100
110		76	130	31	41	26	26	36	144
120		226	.....	110	95	111	75	142	.....
125		.....	.....	165	118	148	105	202	.....
Density, grams per cc. (ASTM D 1217–54)									
130°F.		.....	.....	.....	.....	.....	.....	.....	0.7832
140		0.7774	0.7797	.....	.....	.....	.....	.....	.....
149		.....	.....	0.7819	.....	0.7828	.....	0.7825	.....
150		.....	.....	.....	.....	.....	.....	.....	0.7768
158		.....	0.7736	0.7780	.....	0.7800	.....	.....	.....
160		0.7705	.....	.....	.....	.....	0.7856	.....	.....
176		.....	.....	0.7722	.....	0.7734	0.7806	0.7724	.....
185		.....	.....	.....	0.8027	.....	.....	.....	.....
194		.....	.....	.....	0.8017	.....	.....	.....	.....
Blocking, °F. (Tappi T652 sm 57)	Pick point	96	83	112	117	115	119	112	83
	Blocking point	105	93	119	119	117	121	122	88
Mass spectrometer analysis									
Normal paraffins, %		90.0	61.1	78.3	.....	63.7	48.1	.....	42.5
Isoparaffins, %		10.0	30.1	18.6	.....	31.4	32.1	.....	31.6
Cycloparaffins, %		.....	8.8	2.1	.....	1.2	9.1	.....	25.9
Alkyl Benzenes, %		.....	.....	1.0	.....	0.7	0.7	.....	.....
Total		100.0	100.0	100.0	.....	97.0[c]	90.0[d]	.....	100.0

[a]Drop melt point ASTM D127–49.
[b]Indefinite
[c]3% heavier molecular weight material not volatilized.
[d]10% heavier molecular material not volatilized.

MATERIALS

The materials used in this investigation are identified as follows.

Wax A was prepared in the laboratory by vacuum distilling a commercial paraffin wax to obtain a 6% heart cut of narrow boiling range material.

Waxes B, C, D, and H were commercial petroleum waxes. Wax D was a microcrystalline wax, and all the others were paraffin waxes.

Waxes E and F were made by blending 5 and 25% (weight) of wax D into wax C.

Wax G was made by blending 1% (weight) of a medicinal white oil into wax C. The oil had a viscosity of 340 S.U.S. at 210°F.

The physical properties of the waxes are listed in Table I.

EXPERIMENTAL METHODS

Refractive Index Determinations. The instrument used to determine the refractive indices of the waxes reported in this paper was an Abbe-Valentine (*13, 16, 17, 19, 25, 26*) refractometer. A polaroid disk (*13, 25, 26*) was attached to the eyepiece in such a way that it could be rotated to facilitate reading of the lines seen in the instrument. A sodium vapor lamp was the light source. A temperature-controlled water circulation system was used to regulate the temperature of the prisms in the refractometer. Temperature was measured by means of a thermometer in the water jacket surrounding the upper prism. The prism temperature as indicated by the thermometer generally agreed within 0.2°F. of that given by a copper-constantan thermocouple inserted between the prisms. The thermocouple was used only for calibration.

At the start of the determination the temperature of the refractometer prisms was raised well above the melting point of the wax to be tested. The prisms were separated and cleaned, by wiping first with dry lens paper, and then with paper saturated with hexane. The test wax was melted on a water bath and thoroughly mixed. Several drops were then applied to the hot, dry, lower prism and to the area immediately surrounding it, using a clean glass rod to make the transfer. Care was taken to avoid touching the prism with the rod. Keeping the lower prism nearly horizontal, the prisms were then closed carefully, so as to avoid entrapment of air bubbles between them. Several minutes later, the prisms were separated again, and the surfaces were wiped free of the wax with dry lens paper. This step was included to minimize the effect of contamination by previous samples.

The wax sample was then reapplied and the prisms were closed as before. Care was taken to flood the entire lower prism and the area immediately surrounding it with melted wax. This minimized separation of the solid wax film from the glass as contraction took place on cooling, and thereby made the lines appear more distinct.

The temperature of the sample in the instrument was allowed to decrease slowly to the point at which readings began. This temperature was held for at least 5 minutes, and a reading of the refractive index was taken. Readings were then taken at successively lower temperatures, being spaced at convenient temperature intervals. In the regions where phase changes were taking place, readings were made at closer intervals than elsewhere. The rate of cooling was not permitted to exceed about 2°F. in 5 minutes, and the temperature was held at each point of reading for no less than 5 minutes before the reading was taken.

No difficulty was experienced in reading the lines in the refractometer at temperatures above the melting point of the wax. However, when the wax had solidified the lines became much less distinct, and it was necessary to take three readings and average them to compensate for this. The polaroid disk was used to advantage in taking readings with the wax in the solid state. By suitable rotation of the disk, the boundaries marking the ordinary and extraordinary

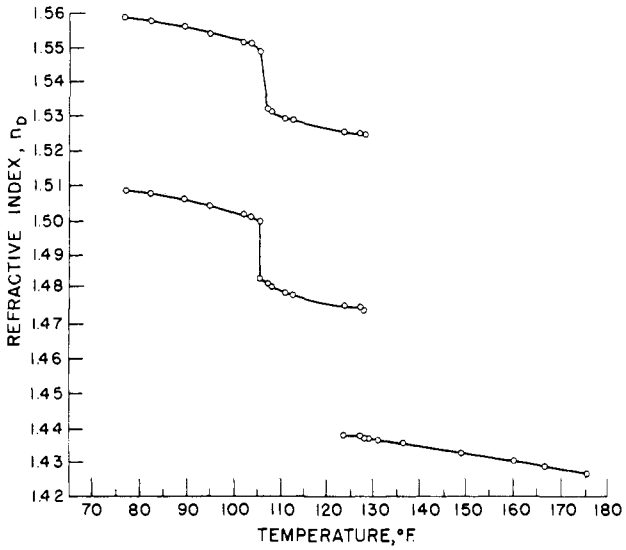

Figure 1. Refractive index vs. temperature for wax A

indices in turn could be sharpened, and the readings facilitated (*13*, *25*, *26*).

Density Measurements. Density of the waxes in the liquid state was determined according to a proposed modification of ASTM Method D 1217-54. In this procedure (*2*, *3*) the liquid sample is weighed in a pycnometer at the desired temperature. The density is then calculated from this weight and the previously determined weight of water required to fill the pycnometer at the same temperature, both weights being corrected for the buoyancy of air.

Melting Point Determinations. Melting points of the paraffin waxes and of the 5 and 25% microcrystalline wax blends were determined according to ASTM Method D 87-42 (*4*). The melting point is the temperature at which melted paraffin wax, when allowed to cool under specified conditions, first shows a minimum rate of temperature change.

Melting point of the microcrystalline wax was determined by ASTM Method D 127-49 (*5*). The melting point is the temperature at which the wax becomes sufficiently fluid to drop from the thermometer used in making the determination under the specified conditions.

Melting points also were estimated from the refractive index data. These points were chosen as the lowest temperature reading before the first appearance of the solid phase.

Table II. Refractive Indices, Densities, and Specific Volumes for Wax A

°F.	n_D	n_o	n_e	d	1/d
149.0	1.4328	.....	.....	0.7744	1.2913
136.4	1.4356	.....	.....	0.7787	1.2842
131.0	1.4365	.....	.....	0.7801	1.2819
129.2	1.4370	.....	.....	0.7809	1.2806
128.3	1.4370	1.4736	1.5243	0.8625	1.1594
123.8	1.4379	1.4752	1.5254	0.8646	1.1566
113.0	.....	1.4782	1.5285	0.8692	1.1505
108.5	.....	1.4804	1.5306	0.8723	1.1464
107.6	.....	1.4817	1.5318	0.8743	1.1438
106.2	.....	1.4995	1.5484	0.9000	1.1111
102.2	.....	1.5016	1.5515	0.9035	1.1068
95.0	.....	1.5040	1.5539	0.9070	1.1025
89.6	.....	1.5060	1.5560	0.9101	1.0988
82.4	.....	1.5075	1.5577	0.9123	1.0961
77.0	.....	1.5084	1.5585	0.9136	1.0946
66.2	.....	1.5108	1.5607	0.9170	1.0905

°F. Fahrenheit.
n_D. Refractive index, liquid state.
n_o. Refractive index, solid state, ordinary rays.
n_e. Refractive index, solid state, extraordinary rays.
d Density (calculated).
1/d Specific volume (calculated).

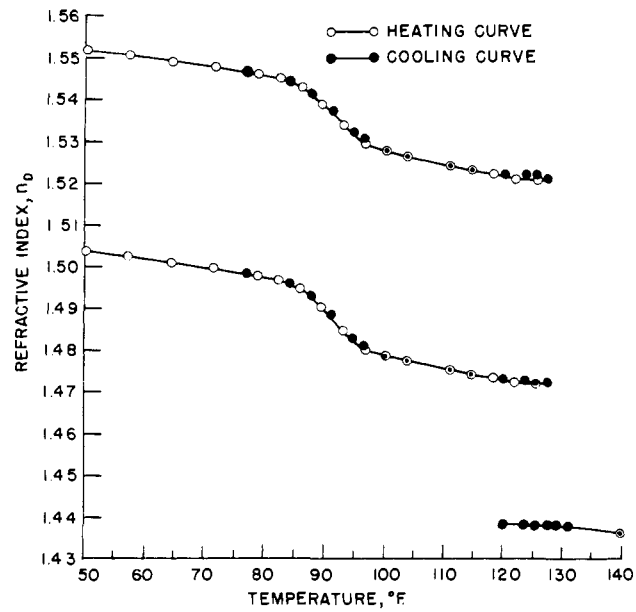

Figure 2. Refractive index vs. temperature for wax B

In this work, readings were taken about 0.5°F. apart in the vicinity of the melting point.

Penetration Tests. The consistencies of the waxes were determined according to a modified form of ASTM Method D 1321-55T (*6*). Consistency is measured by the depth of penetration of a weighted needle into the wax under prescribed conditions. The modification consisted of replacing the standard needle with one having a conical tip 25.4 mm. long and an angle of taper $\frac{9°-25'}{8°-55'}$. The tip is truncated to $\frac{0.16}{0.14}$-mm. diameter. This modification is expected to be approved for inclusion in the standard method (*23*).

Oil Content Determinations. The oil contents of the waxes were determined according to ASTM Method D 721-56T (*7*). The oil content of the wax is defined as the percentage of material that is soluble in methyl ethyl ketone at −25°F. under the specified conditions of test.

Blocking Tests. Blocking may be defined as the temperature at which waxed papers will stick together sufficiently to injure the surface films and affect performance properties. Since blocking may occur over a temperature range, both a "pick point" (initial marring of the film) and a blocking point are measured. A test method for measuring blocking is nearing standardization through cooperative committee work (*1*, *22*).

Mass Spectrometer Analysis. The compositions of the waxes reported in this paper were determined by means of a standard Consolidated Engineering Corp. Model 21-103A analytical mass spectrometer. The instrument was modified for high temperature work using techniques similar to those described by Brown, Melpolder, and Young (*8*).

DISCUSSION OF RESULTS

Although the main purpose of this report is to show how volume changes in a solid petroleum wax can be estimated, the behavior of the refractive index data provides an interesting point for consideration. Consequently, in the discussion which follows, attention is directed frequently toward the results obtained with the refractometer, and how these reflect differences in composition and in the physical properties of the waxes studied.

The relationship between refractive index and temperature for wax A, a close-cut, highly paraffinic wax fraction is shown in Figure 1.

In the diagram, as the temperature decreases, solidification is marked by the appearance of a pair of lines of higher

refractive indices than the liquid line and by the disappearance of the latter. As cooling continues, the wax undergoes a sharp transition to a second solid form which has still higher refractive indices.

Table II gives a partial list of data for refractive index together with calculated densities and specific volumes for wax A.

Figure 2 shows the relationship between refractive index and temperature for wax B, a commercial wax of fairly broad melting range. Here the solid state transition is very

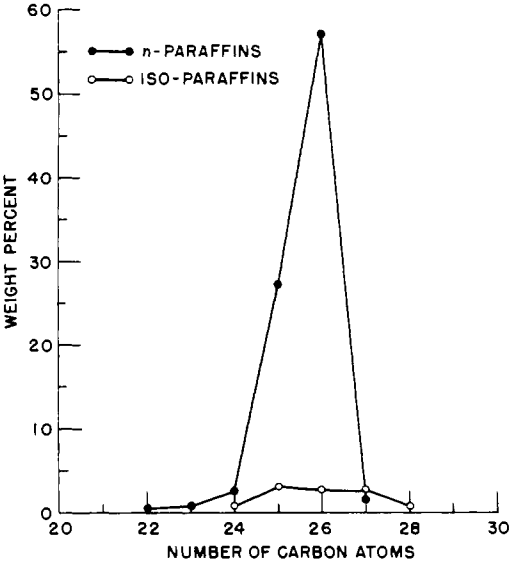

Figure 3. Mass spectrometer analysis of the narrow cut wax A

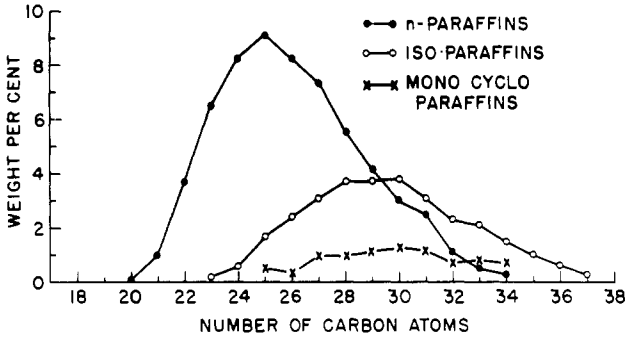

Figure 4. Mass spectrometer analysis of the wide cut wax B

gradual. This may be explained by the presence in wax B of materials whose transition points are distributed over a wide range of temperatures so that a relatively small part of the wax undergoes transition at any given temperature during the cooling process. Wax A does not contain such a distribution of materials.

Mass spectrometer analyses of waxes A and B show this difference in composition (Figures 3 and 4). Wax A has a sharply peaked distribution of normal paraffins and contains also a small amount of isoparaffins. Wax B, on the other hand, shows a broad distribution both in molecular weight and chemical type. The wax analyses are given on a weight per cent basis using calculated weight sensitivities for the parent peaks. The isoparaffins are corrected for fragmentation and reported on the basis of the parent peaks.

The refractive index curves for waxes A and B show persistence of the liquid line for 5° to 7° below the onset of solidification.

In addition to showing the values for refractive index obtained during the normal cooling procedure, Figure 2 shows also the values obtained with wax B in a subsequent warming procedure. Good agreement was obtained between curves

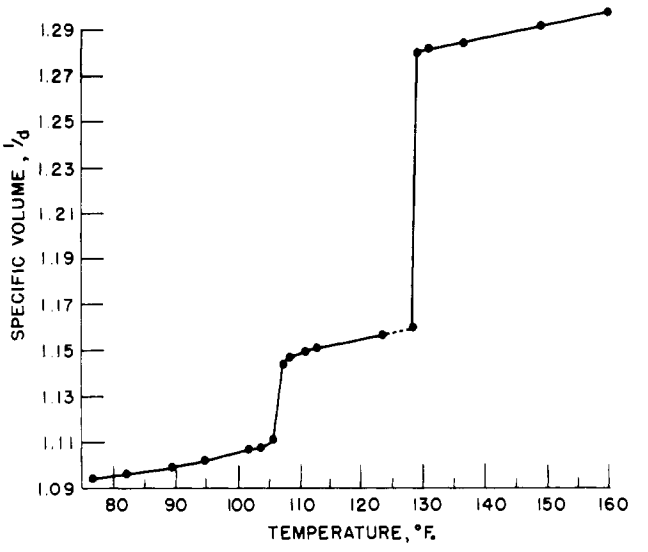

Figure 5. Specific volume vs. temperature for wax A

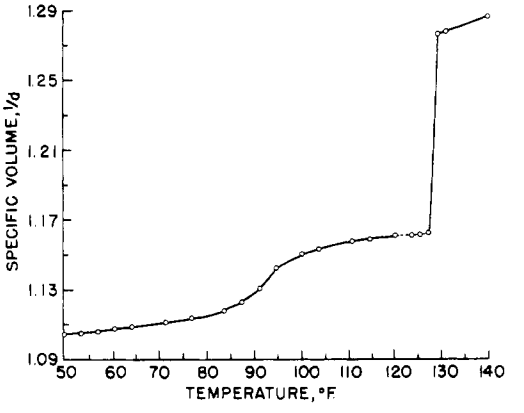

Figure 6. Specific volume vs. temperature for wax B

for heating and cooling the same sample, if sufficient time was allowed for sample and instrument to reach equilibrium.

The relationships between specific volume and temperature for waxes A and B are shown in Figures 5 and 6, respectively. The data used for plotting these curves were calculated from the Lorentz-Lorenz relation as outlined above. Each curve is shown dotted for a few degrees below the melting point to indicate a region of doubt in the calculated specific volumes due to the persistence of the liquid refractive index line in this range. With waxes A and B, the resulting error is very small, but such might not be the case for all waxes. Both of these waxes exhibit a contraction of about 9% on solidification, which occurs over a span of less than 2° F. On further cooling, however, wax A again shows a sharp contraction at the transition point, while the corresponding shrinkage of wax B is very much smoothed out and somewhat smaller in magnitude. It would be expected that the appearance and properties of wax A at room temperature would show the effects of its greater contraction stresses, as compared to wax B. This is the case, for wax A shows considerable cracking and mottling on cooling to room temperature, whether this cooling is rapid or slow, while wax B remains smooth and uniform in structure. Also, the closer packing of the molecules of wax A make it much harder than wax B, particularly at the higher temperatures, as indicated by the penetration values given in Table I.

Refractive index-temperature curves plotted for wax C, a medium width cut, hard, commercial paraffin wax of fairly low oil content and negligible cycloparaffinic content, are shown in Figure 7. The curves show a sharp transition, and are similar to those for wax A, except for the persistence of the liquid line farther below the temperature of initial appearance of the solid lines.

The relationship between refractive index and temperature is shown in Figure 8 for wax D, a deoiled microcrystalline wax of medium plasticity, made from a residuum stock. This wax has a very broad molecular weight distribution, and is believed to be high in cycloparaffins and other nonnormal paraffins, as compared to wax C.

Here the curve for the ordinary ray appears to be continuous with that for the liquid wax. The refractive index readings for this ray were easily obtained, since the line in the refractometer was fairly distinct. At temperatures below 126°F. the corresponding readings for the extraordinary ray were also reasonably clear, but at higher temperatures precise readings were very difficult to get, and the uncertainty in this region is suggested by the dotted portion of

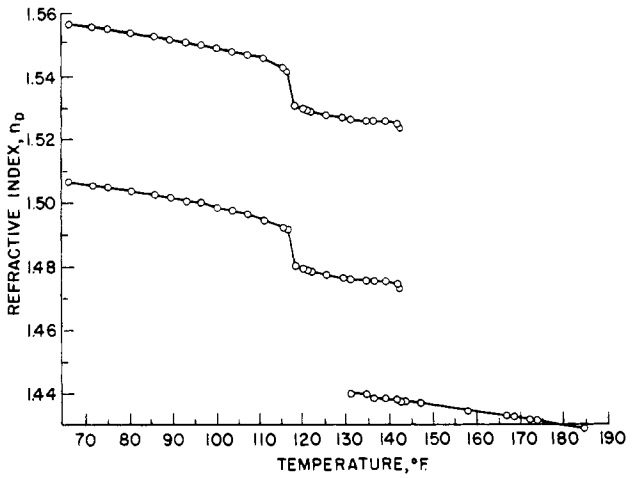

Figure 7. Refractive index vs. temperature for wax C

the curve. The curves for the two rays appear almost to diverge from a point in the region where solidification of the wax occurs.

A possible explanation for the difference in behavior of waxes C and D may be found through consideration of the changes that take place when waxes are cooled from the liquid state. A paraffin wax solidifies by a relatively sudden condensation of its molecules into a dense, oriented form, and this process is helped by the low viscosity of the wax and its relatively narrow molecular weight distribution. The result is the sharp discontinuity in the density (or refractive index) curve for a paraffin wax at its melting point. The microcrystalline wax, on the other hand, has high viscosity and contains molecules in a great variety of sizes and shapes. These molecules may be so hindered in their movements that they are unable to orient themselves quickly into a closely packed arrangement at the average melting point of the wax. They may thus form a slightly oriented

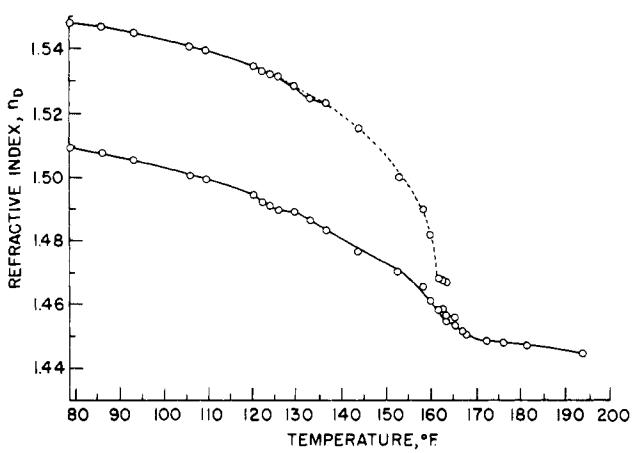

Figure 8. Refractive index vs. temperature for wax D

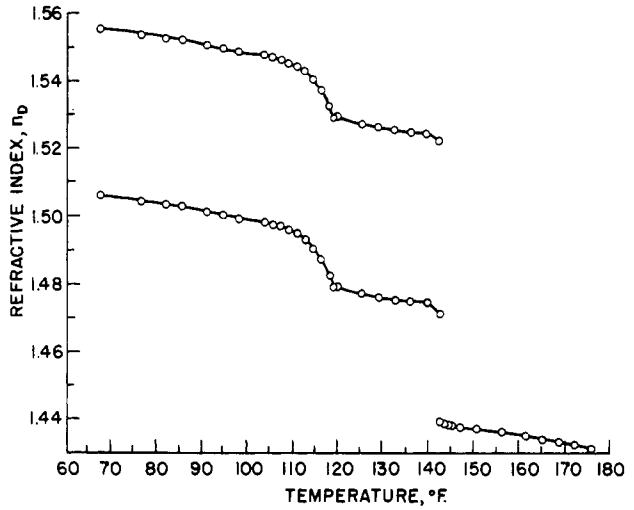

Figure 9. Refractive index vs. temperature for wax E

structure which only gradually becomes more dense as the temperature is lowered.

As the temperature continues to fall, the energies of the paraffin wax molecules drop to a level where a transition to a more closely packed arrangement becomes necessary. Since the molecules are all similar in size and configuration, this transition is quite sudden and nearly complete within a narrow range of temperatures. The microcrystalline wax, on the other hand, contains such a broad distribution of molecular types that transitions, where they occur at all, do so over such a considerable range of temperatures that the effect on observables like refractive index may be totally obscured. It has been reported that the solid state transition disappears for high molecular weight paraffins (*9*, *12*, *21*).

The effect of adding a small amount of microcrystalline wax D to paraffin wax C is illustrated by the curves of Figure 9 for wax E. The liquid line no longer persists below the solidification temperature of the wax, and the curves

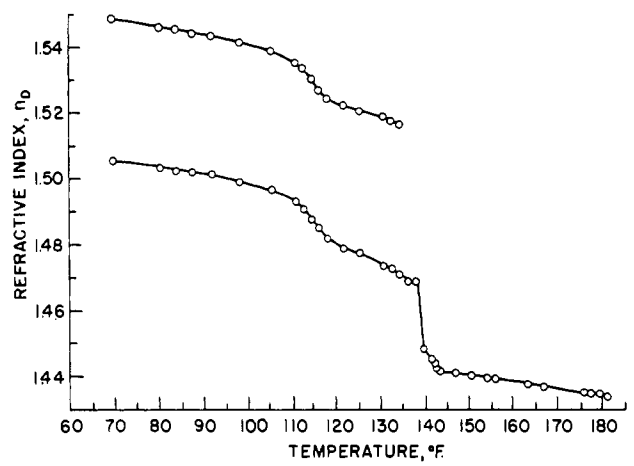

Figure 10. Refractive index vs. temperature for wax F

for the solid wax are slightly distorted at the solidification temperature. While the solid state transition starts abruptly with this wax, the increase of refractive index gradually tapers off, the curve becoming nearly linear again at 13.5°F. below the temperature at which the transition began. Apparently the microcrystalline wax molecules, possibly because they are so different from the paraffin wax molecules in size and shape, break up the orderly arrangement of the lattice and prevent a sudden, uniform condensation to another orderly arrangement. Curves almost identical in shape to those of Figure 9 were obtained for wax G, made by adding 1% of white oil to wax C, the only observable dif-

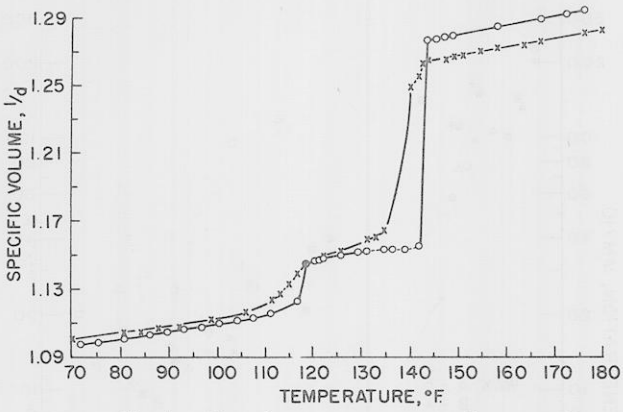

Figure 11. Specific volume vs. temperature for waxes C and F.

o. Wax C
x. Wax F

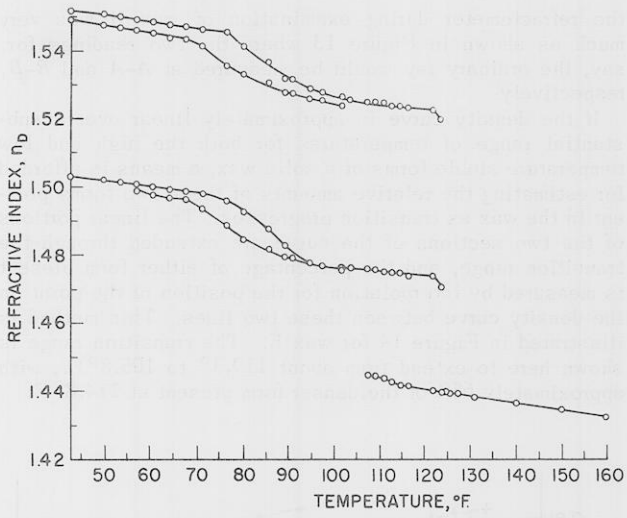

Figure 12. Refractive index vs. temperature for wax H

ference being that wax G showed persistence of the liquid line for about 3° F. below the solidification temperature, which was not the case with wax E. This is a further indication that smoothing out of the transition is caused, in part at least, by the discrepancies in size and shape between the molecules of the additive and those of the base wax.

Wax F, the curves for which are plotted in Figure 10, is similar to wax E, but contains much more microcrystalline wax. This blend shows a further smoothing out of the transition at both the high and low temperature ends of the range. A transition obviously takes place, but probably it would be difficult to observe by ordinary calorimetric methods. Wax F also shows considerable distortion of the refractive index curves in the neighborhood of the solidification point.

The relationships between specific volume and temperature for waxes C and F are shown in Figure 11. It would be expected that waxes showing as great a difference in volume changes with respect to temperature as these two would behave quite differently in use. This is true. A thick coating of wax C on paperboard shatters severely when plunged into cold water, but wax F remains undamaged by the same treatment. Thus wax F should provide a more durable coating for paper containers where low temperature service is involved.

The persistence in the refractometer of the line for the liquid wax after the solid lines have become well established has been noted for wax C, but not for wax E, which contains nearly the same amount of oil and low melting wax. This difference in behavior might be explained in terms of the uniformity of the sample during cooling. At the time that the higher melting components of wax C are beginning to crystallize from the melt, the remaining liquid is still quite free to move. Further crystal formation will preferentially take place on the surface of the existing solid particles with a tendency toward exclusion of liquid components from the crystals. The effect will be a fractional crystallization process, basically the same in principle as that used in commercial deoiling operations. When the wax is nearly solid, the lower melting waxes and oils are sufficiently segregated on the instrument prisms to show a separate liquid line in addition to the solid refractive indices exhibited by the bulk of the sample. With wax E this is not so. The presence of the microcrystalline wax appears to inhibit the migration of liquid components during the solidification process, so that the resultant composition of the solid wax remains uniform, even on a very small scale of observation.

In some instances it has been possible to observe the effect of this assumed fractionation during solidification upon the refractive index changes in the transition region. Figure 12 shows this for wax H, a fairly low melting paraffin

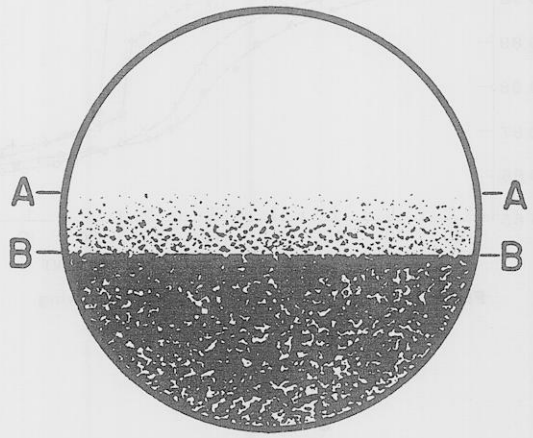

Figure 13. Refractometer field of wax H in the transition range showing fractionation effects

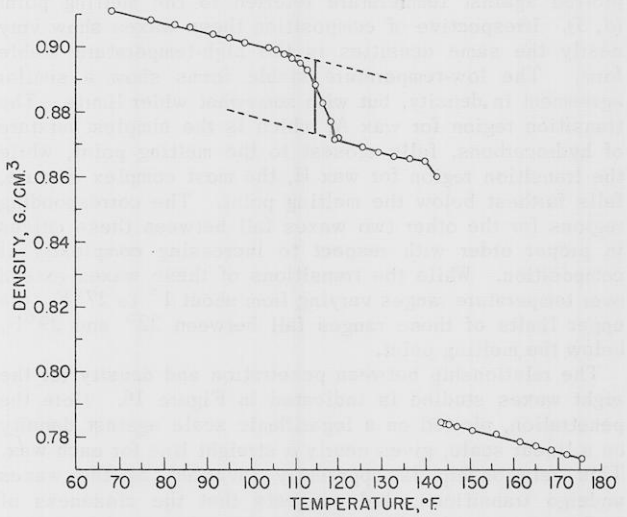

Figure 14. Density-temperature curve for wax E showing estimation of relative amounts of high and low temperature stable forms

wax of broad molecular weight and type distribution. Here the liquid line persists for 16.2° F. below the onset of solidification, indicating some separation of components, and in addition, two curves are shown for each of the solid refractive indices of the wax. These curves are merely boundaries showing the range of refractive index readings obtained for the solid wax. The appearance of the field of

the refractometer during examination of wax H was very much as shown in Figure 13 where the two readings for, say, the ordinary ray would be measured at *A–A* and *B–B*, respectively.

If the density curve is approximately linear over a substantial range of temperatures for both the high and low temperature stable forms of a solid wax, a means is afforded for estimating the relative amounts of these two forms present in the wax as transition progresses. The linear portions of the two sections of the curve are extended through the transition range, and the percentage of either form present is measured by interpolation for the position of the point on the density curve between these two lines. This method is illustrated in Figure 14 for wax E. The transition range is shown here to extend from about 119.3° to 105.8°F., with approximately 65% of the denser form present at 114.8°F.

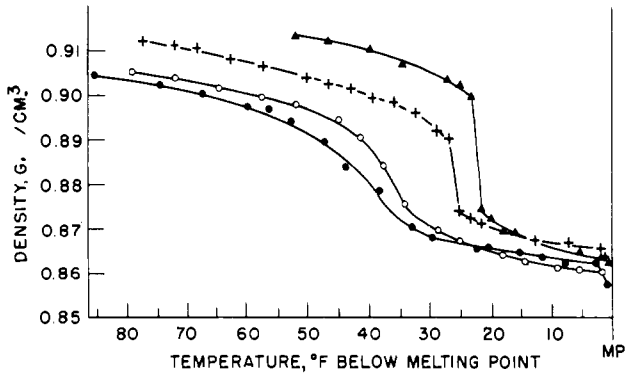

Figure 15. Density-temperature curves showing effect of composition

▲ Wax A
○ Wax B
+ Wax C
● Wax H

In Figure 15 solid densities for waxes A, B, C, and H are plotted against temperature referred to the melting point (*4*, *5*). Irrespective of composition these waxes show very nearly the same densities in the high-temperature stable form. The low-temperature stable forms show a similar agreement in density, but with somewhat wider limits. The transition region for wax A, which is the simplest mixture of hydrocarbons, falls closest to the melting point, while the transition region for wax H, the most complex mixture, falls farthest below the melting point. The corresponding regions for the other two waxes fall between these curves in proper order with respect to increasing complexity of composition. While the transitions of these waxes extend over temperature ranges varying from about 1° to 27°F., the upper limits of these ranges fall between 22° and 29°F. below the melting point.

The relationship between penetration and density for the eight waxes studied is indicated in Figure 16. Here the penetration, plotted on a logarithmic scale against density on a linear scale, gives nearly a straight line for each wax. This relationship is apparently invariant as the waxes undergo transitions, and suggests that the closeness of packing on a molecular scale is of prime importance as a factor affecting the hardness of a wax. The rapid changes in density of waxes undergoing transitions may thus explain the erratic nature of penetration test results obtained at temperatures in or near the transition region, particularly if the wax has very sharp transition characteristics. It would be expected that because densities change sharply when waxes undergo transitions, hardness as measured by the needle penetration test, would show a similar stepwise behavior. Such hardness changes are more difficult to observe than the corresponding density-refractive index changes, because of the slowness with which phase equilibrium is

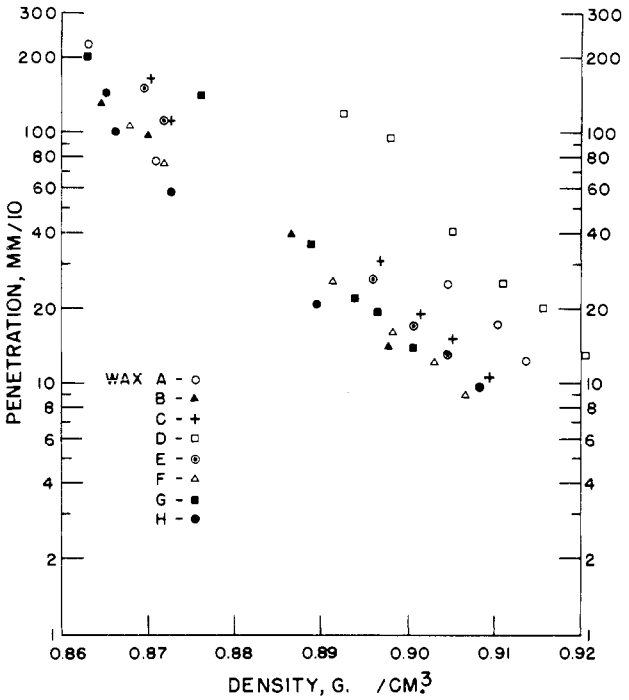

Figure 16. Penetration vs. density

attained in larger wax specimens. The longer time required for completion of transitions in bulky samples is probably also important in its effect on repeatability of penetration results in the transition region, which appears to be associated with penetration values between about 30 and 100 units.

The data of Table I indicate that the blocking temperature of a petroleum wax falls in the transition range, or very close to it. With wide cut waxes such as B and H, blocking occurs at approximately 50% transition, while in the very close cut waxes such as A and C it can be either just below or just above the narrow transition range. In the blends of wax D in wax C the blocking point falls in the upper end of the transition range.

The lack of exact agreement between transition and blocking temperatures, as noted above, may be due in part to difficulties experienced in detecting the blocking point with certain waxes. Perhaps better agreement would be obtained by use of the pressure blocking method of Moyer and Davis (*15*), which has shown certain waxes to be sensitive to pressure applied during the test.

It appears from this study that blocking takes place at a temperature at which transition is sufficiently advanced so that a significant amount of the high temperature stable form, or "soft wax" is present. This would lower the cohesive strength of a wax coating enough to allow transfer of wax from one sheet to another. The rapid expansion in volume during transition could help account for the severe blocking sometimes seen in tightly wound rolls of waxed paper.

ACKNOWLEDGMENT

The authors express their appreciation to the Analytical Division for providing mass spectrometer analyses and physical tests on the waxes used in this study, and to members of the Application Research Division for helping to develop the technique for measuring the refractive indices of the waxes in the solid state.

LITERATURE CITED

(1) Am. Soc. Testing Materials, "ASTM Standards on Petroleum Products and Lubricants," Appendix III, Proposed Method of Test for Blocking Point of Paraffin Wax (November 1955).
(2) *Ibid.*, Appendix VII, Proposed Method of Test for Density and Specific Gravity of Viscous Materials and Melted Solids by Bingham Pycnometer Method (November 1956).

(3) *Ibid.*, Density and Specific Gravity of Liquids by Bingham Pycnometer, ASTM Designation D 1217-54 (November 1956).
(4) *Ibid.*, Melting Point of Paraffin Wax, ASTM Designation D 87-42 (November 1956).
(5) *Ibid.*, Melting Point of Petrolatum and Microcrystalline Wax, ASTM Designation D 127-49 (November 1956).
(6) *Ibid.*, Needle Penetration of Petroleum Waxes, ASTM Designation D 1321-55T (November 1956).
(7) *Ibid.*, Oil Content of Petroleum Waxes, ASTM Designation D 721-56T (November 1956).
(8) Brown, R. A., Melpolder, F. W., Young, W. S., *Petroleum Processing* 7 No. 2, 204 (1952).
(9) Fontana, B. J., *J. Phys. Chem.* 57, 222 (1953).
(10) Gibb, T. R. P., "Optical Methods of Chemical Analysis," p. 338, McGraw-Hill, New York, 1942.
(11) Glasstone, S., "Textbook of Physical Chemistry," p. 528, Van Nostrand, New York, 1948.
(12) Gray, C. G., *J. Inst. Petrol.* 29, 226 (1943).
(13) Johnson, J. F., *Ind. Eng. Chem.* 46, 1046 (1954).
(14) Kolvoort, E. C. H., *J. Inst. Petrol. Technologists* 24, 338 (1938).
(15) Moyer, H. C., Davis, R. R., *Tappi* 38, 473 (1955).
(16) Page, J. M., Jr., *Ind. Eng. Chem.* 28, 856 (1936).
(17) *Ibid.*, 29, 846 (1937).
(18) Pope, *J. Chem. Soc.* 69, 1531 (1896).
(19) Seyer, W. F., Fordyce, R., *J. Am. Chem. Soc.* 58, 2029 (1936).
(20) Seyer, W. F., Morris, W. J., *Ibid.*, 61, 1114 (1939).
(21) Seyer, W. F., Patterson, R. F., Keays, J. L., *Ibid.*, 66, 179 (1944).
(22) Technical Association of the Pulp and Paper Industries, *Tappi* 40, 186A (1957).
(23) TAPPI-ASTM Technical Committee on Petroleum Wax, Meeting, New York, N. Y., February, 1957.
(24) Templin, P. R., *Ind. Eng. Chem.* 48, 154 (1956).
(25) West, C. D., *Ind. Eng. Chem., Anal. Ed.* 10, 627 (1938).
(26) West, C. D., *J. Am. Chem. Soc.* 59, 742 (1937).
Received for review October 18, 1957. Accepted February 15, 1958.

Further Bridged Sulfur Compounds of the Kerosine Boiling Range of Middle East Distillates

STANLEY F. BIRCH, THOMAS V. CULLUM, and RONALD A. DEAN
Research Station, The British Petroleum Co., Ltd., Sunbury-on-Thames, Middlesex, England

Earlier (*1*) an account was given of the identification of a number of thiophenes and mono- and polycyclic sulfides in the sulfurous oil obtained in the process of refining Middle East (Agha Jari) kerosine. Of special interest were two of the sulfides which were solids, possessing a structure in which a carbon ring is bridged by a sulfur atom. The probable presence of other sulfides of similar structure was indicated and further work has now confirmed their presence. The compounds identified, either tentatively or definitely, are listed in Table I; several possess the atomic-bridged structure. Although two polycyclic sulfides, thianaphthene (*12*) and 1,8-dimethyldibenzothiophene (*6*), have been identified in crude oils and also some hydrocarbons possessing an atomic-bridged structure (*11*), these are the only sulfur compounds of this type that have so far been identified in naturally occurring materials. It is of interest, however, to compare their structure with those of the tropane group of alkaloids—e.g., tropane and granatanine.

PREPARATION OF CLOSE BOILING FRACTIONS

The preparation, in the refinery, of the sulfur compound concentrate used in this investigation has been fully described (*1*). Subsequent processing and precise fractional distillation of a portion of this concentrate were also described, and three fractions obtained by this process (XX, XXIV, XXVII, Table II) have been re-examined in the course of this work. In addition a further portion of the sulfur compound concentrate was fractionally distilled to obtain a quantity (15 liters, n_D^{20} 1.4811) of material in the 180° to 192°C. range. Following Dualayer solutizer treatment (*8*) to remove mercaptans, fractionation with 0.7*M* aqueous mercuric acetate solution (*1*) (five extractions each of 25 volume %) yielded, after regeneration of the extracts, a bicyclic sulfide concentrate, 2.5 kg., n_D^{20} 1.4856, which was distilled through a 100-plate column under reduced pressure. The fractions from this distillation (A–I, Table III) were used to obtain concentrates of polycyclic sulfides. Distillation, under reduced pressure, of the raffinate from this extraction left a residue of the same acetoxymercurithiophenes as those described previously (*1*).

CONCENTRATION OF POLYCYCLICS PRESENT IN CLOSE-BOILING FRACTIONS

Because the primary objective was to investigate the polycyclic compounds, the first need was to separate these from the associated monocyclic compounds, which were in general the largest component of the fractions. An attempt to separate mono- and bicyclic compounds by elution chromatography using alumina was only partially successful and similar results were obtained with the corresponding sulfones. The methods finally used were based on the use of the mercury salt complexes of the sulfides, the first stage being fractional extraction with aqueous mercuric acetate solution. It was shown that the previously used method, involving a two-stage acid regeneration (*1*), caused some decomposition of the polycyclic sulfides—e.g., a portion of the tar oil, boiling point, 193°C., was refluxed for 2 hours with aqueous mercuric acetate solution and regenerated by the addition of hydrochloric acid; the loss of bicyclic sulfides was indicated by a fall in refractive index, n_D^{20}, from 1.4932 to 1.4872. The process of fractionation had therefore to depend entirely upon the selectivity of the extraction process.

The fraction was extracted with an amount of aqueous mercuric acetate solution, sufficient only to extract a small percentage of the sulfides, by vigorous agitation, preferably with a high-speed stirrer, for 10 minutes. After water-washing to remove the mercuric acetate complexes remaining dissolved in the sulfide layer, the combined extracts were regenerated by addition to a refluxing aqueous solution of sodium sulfide, followed by removal of the steam-distilled sulfides using an oil-water separator. The raffinate was similarly extracted with further small quantities of mercuric acetate solution until the refractive index of the regenerated sulfide showed that it contained only a small amount of bicyclic compound. By retreatment of bulked fractions it was possible to obtain materials of high refractive index consisting essentially of polycyclic compounds. While recovery of polycyclic sulfides by this procedure was incomplete, the concentrates obtained were undoubtedly representative of the types present, as little separation of individual polycyclics appears to occur during this process.

A further method for the concentration of polycyclic sulfides was based upon the formation and separation of the mercuric chloride complexes. It had been observed that the mercuric chloride complexes of synthetic bicyclic sulfides were almost invariably extremely insoluble and it was found that the least soluble portion of the complexes formed from the tar oil fractions or concentrates (using a high molar ratio of mercuric chloride to sulfide) contained a high proportion of bicyclic sulfides. By further crystal-